AD_____

Award Number: DAMD17-02-1-0142

TITLE: Vitamin D Treatment of Prostate Cancer: The Inhibitory Role of IGFBP-3

PRINCIPAL INVESTIGATOR: David Feldman, M.D.

CONTRACTING ORGANIZATION: Stanford University
Stanford, CA 94305-5401

REPORT DATE: February 2004

TYPE OF REPORT: Annual

PREPARED FOR: U.S. Army Medical Research and Materiel Command
Fort Detrick, Maryland 21702-5012

DISTRIBUTION STATEMENT: Approved for Public Release;
Distribution Unlimited

The views, opinions and/or findings contained in this report are those of the author(s) and should not be construed as an official Department of the Army position, policy or decision unless so designated by other documentation.

REPORT DOCUMENTATION PAGE

Form Approved OMB No. 074-0188

1. AGENCY USE ONLY (Leave blank)	2. REPORT DATE	3. REPORT TYPE AND DATES COVERED
	February 2004	Annual (15 Jan 2003 - 14 Jan 2004)

4. TITLE AND SUBTITLE

Vitamin D Treatment of Prostate Cancer: The Inhibitory Role of IGFBP-3

5. FUNDING NUMBERS

DAMD17-02-1-0142

6. AUTHOR(S)

David Feldman, M.D.

7. PERFORMING ORGANIZATION NAME(S) AND ADDRESS(ES)

Stanford University
Stanford, CA 94305-5401

E-Mail: feldman@cmgm.stanford.edu

8. PERFORMING ORGANIZATION REPORT NUMBER

9. SPONSORING / MONITORING AGENCY NAME(S) AND ADDRESS(ES)

U.S. Army Medical Research and Materiel Command
Fort Detrick, Maryland 21702-5012

10. SPONSORING / MONITORING AGENCY REPORT NUMBER

11. SUPPLEMENTARY NOTES

12a. DISTRIBUTION / AVAILABILITY STATEMENT

Approved for Public Release; Distribution Unlimited

12b. DISTRIBUTION CODE

13. ABSTRACT (Maximum 200 Words)

Calcitriol plays a critical role in maintaining mineral homeostasis but also exhibits antiproliferative activity in many cancers. We have shown that the antiproliferative actions of calcitriol in the LNCaP human prostate cancer (PCa) cell is mediated in large part by induction of insulin-like growth factor binding protein–3 (IGFBP-3). The purpose of this study was to determine the molecular mechanism involved in calcitriol regulation of IGFBP-3 and to identify the putative vitamin D response element (VDRE) in the IGFBP-3 promoter. We cloned 6 kb of the IGFBP-3 promoter and demonstrated its responsiveness to calcitriol in transactivation assays. Computer analysis identified a putative VDRE between -3296/-3282 that is similar to other known VDREs. In gel shift assays the vitamin D receptor (VDR) showed strong calcitriol-dependent binding to this putative VDRE. ChIP assay demonstrated that calcitriol recruited the VDR/RXR heterodimer to the VDRE site. In transactivation assays the VDRE promoter was induced 2-fold by calcitriol. Mutations created in the VDRE resulted in a loss of IGFBP-3 induction confirming the critical VDRE sequence. In conclusion, we have identified a functional VDRE in the distal region of the human IGFBP-3 promoter that directly mediates the action of calcitriol.

14. SUBJECT TERMS

vitamin D, calcitriol, prostate cancer, vitamin D receptor, VDRE, IGFBP-3, antiproliferation, androgens, treatment

15. NUMBER OF PAGES

22

16. PRICE CODE

17. SECURITY CLASSIFICATION OF REPORT	18. SECURITY CLASSIFICATION OF THIS PAGE	19. SECURITY CLASSIFICATION OF ABSTRACT	20. LIMITATION OF ABSTRACT
Unclassified	Unclassified	Unclassified	Unlimited

Table of Contents

INTRODUCTION

We have previously shown that calcitriol (1,25-dihydroxyvitamin D_3) the active hormonal form of vitamin D, is antiproliferative in several prostate cancer (PCa) models including human prostate cancer cell lines (1-3). This has led us to hypothesize that calcitriol may be a useful therapy for PCa (4). In studies of the LNCaP human PCa cell line, we further demonstrated that calcitriol induction of insulin-like growth factor binding protein–3 (IGFBP-3) was necessary for the antiproliferative activity (5). The IGFBP-3 gene appears to mediate the antiproliferative activity of calcitriol by inducing a subsequent gene, p21, an inhibitor of the cell cycle. Prevention of IGFBP-3 expression, using antibodies to immunoneutralize IGFBP-3 or antisense to prevent IGFBP-3 mRNA transcription, abrogated the antiproliferative activity of calcitriol and the induction of p21. We therefore concluded that induction of IGFBP-3 is the critical step in calcitriol's antiproliferative activity in the LNCaP cells (5).

IGFBP-3 is the major binding protein for circulating IGF-1, a potent mitogen (6). IGFBP-3 has activities that are antimitogenic because it sequesters IGF-1. However, it has recently become clear that IGFBP-3 also has IGF-independent actions that are antiproliferative and proapoptotic (7). These activities make IGFBP-3 a potentially important factor in halting cancer cell growth (5, 8, 9). The circulating blood level of IGFBP-3 has also been studied as a potential marker of PCa risk (10)

The goal of the current project is to further investigate the role of IGFBP-3 in the antiproliferative actions of vitamin D in PCa. Calcitriol regulates target genes by binding to the vitamin D receptor (VDR) (11). The calcitriol-bound VDR dimerizes with retinoid X receptor (RXR) and this complex then binds to a vitamin D regulatory element (VDRE) in the promoter region of target genes (12). Therefore, to study the vitamin D regulation of IGFBP-3, we set out to determine whether a VDRE was present in the promoter region of the IGFBP-3 gene.

In addition, we hoped to resolve another controversy about the nature of calcitriol regulation of the critical gene, p21. This gene is a cyclin-dependent kinase (Cdk) inhibitor and an important regulator of the cell cycle and cell proliferation. In our studies, calcitriol appeared to regulate IGFBP-3 that then regulated p21. In contrast, the studies of Liu et al (13) concluded that calcitriol directly regulated p21. The differences could be resolved, at least partially, by demonstrating a VDRE in the IGFBP-3 promoter region and demonstrating direct regulation of IGFBP-3 by calcitriol.

BODY

CALCITRIOL REGULATION OF IGFBP-3 BY A VDRE

In our Statement of Work, our major goal was to investigate the regulation of IGFBP-3 by calcitriol in PCa cells. In previous work, we have clearly demonstrated that calcitriol's antiproliferative actions in some PCa cells are mediated by induction of IGFBP-3 (5). Thus, it is possible that a VDRE exists in the IGFBP-3 promoter to directly regulate the effect of calcitriol on IGFBP-3.

The second goal of this project is to determine the molecular mechanism of calcitriol's action on IGFBP-3. To study this we performed the following

experiments. The figures and Table will be found in the copy of the paper appended to this report.

Induction of IGFBP-3 mRNA by 1,25-(OH)2D3 in LNCaP Cells

We have previously shown that treatment of LNCaP cells with 1–1000 nM of 1,25-(OH)2D3 for 48 h caused a 1.3- to 2.9-fold increase of IGFBP-3 at both message and protein levels (5). To further elucidate the mechanism for 1,25-(OH)2D3 induction of IGFBP-3, we performed a time course of IGFBP-3 mRNA expression in LNCaP cells treated with 10 nM 1,25-(OH)2D3. As shown in Fig. 1 (see appended paper from Molecular Endocrinology), at 6 h IGFBP-3 mRNA is induced 2.7-fold in the 1,25-(OH)2D3-treated cells. At 12 h, the IGFBP-3 mRNA peaks and remains elevated after 48 h, which is consistent with our previous report (5). The IGFBP-3 protein level is increased approximately 3-fold after 48 h achieving concentrations of 3–6 ng/ml in the conditioned medium of 1,25-(OH)2D3-treated LNCaP cells (5). These results suggest that 1,25-(OH)2D3 may directly regulate the transcription of IGFBP-3 in LNCaP cells. Although growth inhibition by exogenously added IGFBP-3 appears to require 10–100 ng/ml of the protein, the intracrine as well as paracrine effects of endogenously synthesized IGFBP-3 induced by 1,25-(OH)2D3 appear to be sufficient to cause growth inhibition (5).

To determine whether 1,25-(OH)2D3 is involved in the transcriptional regulation of the IGFBP-3 gene in LNCaP cells, we cloned a PCR fragment containing approximately 1.9 kb of the published IGFBP-3 promoter sequence (–1901 to +55) into the promoterless luciferase reporter vector, pGL3-basic. We then cotransfected this construct with a VDR expression vector (pSG5-VDR) into LNCaP and HeLa cells. As shown in Fig. 2 (appended), the 1.9-kb fragment showed no stimulation by 1,25-(OH)2D3 in either cell line. We then used the published sequence to search the GenBank database to obtain more 5' flanking sequence. Based on our search, we generated further upstream sequence of the IGFBP-3 promoter by PCR. A DNA fragment from –1901 to –3595 was ligated to the –1901 construct, generating a promoter sequence from –3595 to +55. In transactivation assays, this promoter sequence showed approximately 2-fold induction by 1,25-(OH)2D3 in both LNCaP and HeLa cells (Fig. 2). No further increase in 1,25-(OH)2D3 transactivation was observed when sequences up to –5992 were tested. These results suggest that a putative VDRE is present in the region from –3595 to –1901 of the IGFBP-3 promoter.

Identification of a Functional VDRE in the Distal Promoter of the IGFBP-3 Gene

To determine whether the sequence between –3590 and –1901 can act as an enhancer element, the sequence from –3590 to –1753 was cloned 5' of the heterologous simian virus 40 (SV40) promoter in the pGL3-promoter vector. LNCaP and HeLa cells were cotransfected with this chimeric construct and pSG5-VDR and then treated with 10 nM 1,25-(OH)2D3. As shown in Fig. 3A, the sequence from –3590 to –1753 showed an increase in SV40 promoter activity of about 1.8-fold in LNCaP and 2.5-fold in HeLa cells, demonstrating 1,25-(OH)2D3 responsiveness by this 1.8-kb fragment.

To further define the VDRE within this 1.8-kb fragment of the IGFBP-3 promoter, deletions were generated, cloned into the pGL3-promoter vector and then transfected into HeLa cells. As shown in Fig. 3B, removal of the 3' sequence from –1753 to –2474 did not change the enhancer activity. Further deletions from –2950 to –2474 and from –3205 to –2950 displayed similar enhancer activity. The data suggest that a VDRE is located in the 386-bp fragment between –3590 and –3205. Additional deletions within this fragment were made to characterize the minimal enhancer sequence (Fig. 3B). When the 5' sequence was further deleted from –3590 to –3410, the activity remained the same as the –3590/–3205 construct. Further 3' deletion from –3410 to –3205, however, resulted in complete loss of the enhancer activity. The data suggest that the VDRE is located within this 206-bp fragment between –3410 and –3205.

The VDREs are generally composed of two direct repeats of six bases separated by a three-nucleotide spacer referred to as a DR3 motif. Computer analysis of the 206-bp fragment identified a potential VDRE (GGTTCA ccg GGTGCA) located between –3296 and –3282. We refer to this 15-bp sequence as BP3-VDRE. This sequence contains two hexameric core sites separated by three nucleotides resembling a DR3 motif. As shown in Table 1, the BP3-VDRE is 92% identical with the distal VDRE of the rat 24-hydroxylase promoter located at –259 (designated r24-OHdistal VDRE) and 87% identical with the VDRE consensus sequence.

Confirmation of VDRE Properties by EMSA

We used EMSA to determine whether the VDR can bind to the putative IGFBP-3 VDRE sequence. Double-stranded BP3-VDRE and r24-OH distal VDRE oligonucleotides were incubated with crude cell extracts from COS-7 cells transfected with pSG5 or pSG5-VDR vectors. A strong specific DNA-protein complex with the VDR-transfected cell extracts was observed both with probe BP3-VDRE (Fig. 4B, lane 4) and with probe r24-OHdistal VDRE (data not shown). This binding activity was highly induced by 10 nM of 1,25-(OH)2D3 (Fig. 4B, lane 5). A complex with identical mobility to the VDR-transfected cell extracts was also observed with the empty vector-transfected cell extracts (Fig. 4B, lane 2); however, it was not induced by 1,25-(OH)2D3 (Fig. 4B, lane 3). When a 200-fold molar excess of unlabeled oligonucleotide, either BP3-VDRE or r24-OHdistal VDRE, was added, the signal was diminished (Fig. 4B, lanes 6 and 7). In contrast, when an unlabeled oligonucleotide containing mutations in either the 5' (BP3-VDREm1) or the 3' (BP3-VDREm2) hexamic sequence (Fig. 4A) was added, the DNA-binding was no longer competed (Fig. 4B, lanes 8 and 9). These results indicate that the BP3-VDRE sequence may be similar to the r24-OH distal VDRE that binds the nuclear proteins VDR and RXR.

To confirm the presence of VDR and protein in the BP3-VDRE complex, VDR or RXR antibodies were added for supershift assays. As shown in Fig. 4C, the BP3-VDRE sequence was bound by proteins recognized by VDR or RXR antibodies, thus producing supershifted complex SS1 (lane 3) or complex SS2 (lane 4), respectively. Both complexes SS1 and SS2 were of similar mobility to that seen with the r24-OHdistal VDRE probe (data not shown).

Confirmation of VDRE Properties by Chromatin Immunoprecipitation (ChIP) Assay

ChIP assays were performed to further prove that 1,25-(OH)2D3 was capable of recruiting VDR/RXR to the chromatinized BP3-VDRE in the native IGFBP-3 promoter in the absence of VDR overexpression. LNCaP cells were treated with or without 1,25-(OH)2D3 and then subjected to ChIP assay. PCR was performed with the purified immunoprecipitated chromatin DNA using the primers designed to amplify the IGFBP-3 promoter sequence encompassing BP3-VDRE. As shown in Fig. 5, with the antibody against VDR (lanes 5 and 6) or RXR (lanes 7 and 8) added in the immuoprecipitation reaction, an expected size band was produced only in the 1,25-(OH)2D3-treated cells (lanes 6 and 8), indicating that the BP3-VDRE is the interacting sequence with the VDR/RXR complex. The results further confirm a functional VDRE site in the natural chromatin structure in the intact cells. Therefore, our EMSA and ChIP assay results strongly indicate that the BP3-VDRE sequence in the human IGFBP-3 promoter is a novel VDR binding element.

Confirmation of Enhancer Activity of the BP3-VDRE by Transactivation

To determine whether the BP3-VDRE sequence acts as an enhancer in a 1,25-(OH)2D3 inducible fashion, a single copy of this sequence was cloned into the pGL3-promoter expression vector upstream of the heterologous SV40 promoter in both sense and antisense orientations (Fig. 6). LNCaP cells cotransfected with the BP3-VDRE/SV40 promoter chimeric constructs and pSG5-VDR showed approximately 2-fold induction of luciferase activity in the presence of 10 nM 1,25-(OH)2D3 as compared with the cells without 1,25-(OH)2D3. This increase occurred whether the BP3-VDRE was in the sense or antisense orientation. The pGL3-promoter empty vector showed no 1,25-(OH)2D3 induction (data not shown). The mutations (Fig. 4A) in the RXR-binding site (m1) or VDR-binding site (m2) of the BP3-VDRE enhancer, which disrupt VDR/RXR binding in the EMSA study (Fig. 4B), were also introduced into the BP3-VDRE/SV40 promoter hybrid construct. As shown in Fig. 6, both mutants m1 and m2 resulted in loss of 1,25-(OH)2D3 inducibility, indicating that the two hexameric sequences are required for the enhancer activity of the BP3-VDRE. To reveal whether BP3-VDRE functions in the same manner in both the native promoter and the heterologous SV40 promoter, the same mutations (m1 or m2) were introduced into the –5992/+55 native promoter reporter construct. Neither mutant showed induction by 1,25-(OH)2D3 that is comparable to the mutated heterologous promoter construct (Fig. 6).

A single copy of wild-type BP3-VDRE sequence in either the sense (wt-s) or antisense orientation (wt-as), as well as mutated BP3-VDRE (m1 or m2) in the antisense direction, was cloned into the pGL3-promoter reporter vector. The m1 and m2 oligonucleotides are the same as used in the EMSA (Fig. 4A). The m1 oligonucleotide has a mutation in the RXR binding site (), whereas the m2 contains a mutation in the VDR binding site (). The same mutations were also introduced into the –5992/+55 pGL3-Basic reporter construct. Either the heterologous or the natural promoter constructs were cotransfected with pSG5-VDR into LNCaP cells and treated with ethanol or 10 nM 1,25-(OH)2D3 for 16–18 h. The activity of each construct is expressed as fold induction over control. Data are representative of three independent experiments, each performed in triplicate.

OTHER GOALS OF THE RESEARCH REGARDING IGFBP-3 Regulation

Androgen/calcitriol interactions

Another goal of this project is to study the interaction of androgens and calcitriol in regulating target genes including IGFBP-3. Using real-time PCR, we showed that androgen treatment (R1881) alone increased IGFBP-3 mRNA about 3-fold. However, androgen together with calcitriol resulted in a remarkable increase of over 25-fold indicating a synergistic effect of androgen and calcitriol on IGFBP-3 regulation. In transactivation assays, the 6 kb IGFBP-3 promoter sequence responded to calcitriol or androgen treatment. The combination of androgen and calcitriol doubled the effect of either hormone alone. Whether this induction of IGFBP-3 by androgen is a direct or indirect effect remains to be determined. Currently this study is in progress using the IGFBP-3 reporter constructs described above.

Retinoids, PPARs and HDAC inhibitors

We have also studied the interaction of other important regulators including 9-cis retinoic acid [(9 cis-RA), the RXR ligand], rosiglitazone [a peroxisome proliferator-activated receptor (PPAR)γ ligand], and tricostatin A [TSA, a histone deacetylase (HDAC) inhibitor] using Northern blot analysis as well as our established IGFBP-3 promoter-reporter transactivation system. We found that all of these regulators significantly enhanced calcitriol's upregulation of IGFBP-3 expression. These findings suggest that these agents given in combination with calcitriol would increase calcitriol's antiproliferative activity. It is possible that combination therapy would allow the use of lower doses of calcitriol to achieve a therapeutic antiproliferative effect and thereby diminish the hypercalcemic side-effects of calcitriol in prostate cancer therapy.

Regulation of IGFBP-3 by calcitriol analogs

Another goal of the project was to evaluate IGFBP-3 regulation by several calcitriol analogs that are less hypercalcemic than calcitriol. In other words, we wanted to know whether ability to induce IGFBP-3 could be used to explore the antiproliferative activity of the calcitriol analogs on PCa cells. To establish this assay, we measured both the effect of the analogs on PCa cell proliferation as well as real-time PCR to assess the analog's ability to induce IGFBP-3. We used LNCaP cells for both the growth studies and the IGFBP-3 induction. Analogs EB1089, Ro24-5531, KH1060 and Ro27-0574, each at 10 nM, resulted in over 10-fold increase in IGFBP-3 mRNA compared to the vehicle treatment. The analogs inhibited cell proliferation by over 65%. In comparison, 10 nM calcitriol induced a 2-3 fold of induction of IGFBP-3 mRNA and about 55% inhibition of cell growth. The studies indicate that these analogs have a higher potency than calcitriol at both IGFBP-3 induction and antiproliferative activity.

KEY RESEARCH ACCOMPLISHMENTS

- Identified the presence of a VDRE in the IGFBP-3 promoter.
- Proved that calcitriol directly regulates IGFBP-3.
- Demonstrated that calcitriol indirectly regulates p21and the effect is mediated

through IGFBP-3 induction.

- Characterized an important VDRE with unique characteristics in an important calcitriol target gene.
- Provided information on the promoter region of the IGFBP-3 gene.
- Established an advanced biotechnique, the ChIP assay, to study DNA-protein interactions in our lab that will be very useful to study additional hormone receptor-DNA interactions.
- Demonstrated the induction of IGFBP-3 via action on its promoter by other important regulators including androgens, retinoids, PPAR ligands and HDAC inhibitors.
- Evaluated the potency of several less hypercalcemic calcitriol analogs to induce IGFBP-3 and concurrently their ability to be antiproliferative in PCa cells.
- Provided data on possible approaches to combination therapy that would improve the therapeutic potency of calcitriol in PCa therapy.
- Clones of our IGFBP-3 promoter have been requested by several labs working in this field. We have supplied our reporter fragments to all labs that have requested the materials.

REPORTABLE OUTCOMES

All of the above mentioned research accomplishments are reportable. We have written one publication describing the identification of a functional VDRE in the IGFBP-3 promoter that has recently been published in Molecular Endocrinology 18:1109-1119,2004 (appended to this report). Other outcomes will be brought to publication stage during the next year of the grant.

CONCLUSIONS

This research has elucidated the presence of a VDRE in the promoter region of the IGFBP-3 gene. This finding establishes the fact that calcitriol directly regulates IGFBP-3 via a classical VDRE. Since only a modest number of VDREs have been characterized, this finding adds to the series of known VDREs and provides useful data for further elucidation of additional VDREs. The research also demonstrates how this critical gene is regulated and provides DNA sequence data for the IGFBP-3 promoter region to support further analysis of additional regulators or modulators of IGFBP-3 gene expression. Most importantly, the work clarifies how calcitriol induces this most important regulator of PCa cell growth.

This study has also demonstrated enhanced calcitriol action to induce IGFBP-3 by other important regulators including androgen, retinoid, rosiglitazone and HDAC inhibitor and has evaluated the potency of several calcitriol analogs with less

hypercalcemic activity. The results have provided new insights into improving calcitriol's therapeutic efficacy in PCa therapy.

As detailed in the original grant, we plan to evaluate the IGF/IGFBP-3 axis in several PCa cell lines and study the nuclear mechanisms of IGFBP-3 interaction with RXR and VDR to inhibit PCa cell growth.

RESPONSE TO RECOMMENDATIONS FOR REVISION

1. Comprehensive Data have been added to the body of the report as requested.

2. Reportable outcomes include the manuscript published in Molecular Endocrinology that is appended to this report.

3. Progress delays include two items. First, the VDRE in IGFBP-3 is over 3,000 base-pairs upstream of the start site. This is further away from the start site than any other VDRE identified to date. To find it and characterize it required cloning large amounts of new DNA and searching for the appropriate region. Second, during the conduct of this research, the ChIP assay was popularized as a uniquely useful method to confirm the nature of functional regulatory elements. This method had to be developed in our laboratory. It is now routinely performed by us.

REFERENCES

1. Skowronski RJ, Peehl DM, Feldman D 1993 Vitamin D and prostate cancer: 1,25 dihydroxyvitamin D3 receptors and actions in human prostate cancer cell lines. Endocrinology 132:1952-60
2. Peehl DM, Skowronski RJ, Leung GK, Wong ST, Stamey TA, Feldman D 1994 Antiproliferative effects of 1,25-dihydroxyvitamin D3 on primary cultures of human prostatic cells. Cancer Res 54:805-10
3. Skowronski RJ, Peehl DM, Feldman D 1995 Actions of vitamin D3, analogs on human prostate cancer cell lines: comparison with 1,25-dihydroxyvitamin D3. Endocrinology 136:20-6
4. Zhao XY, Feldman D 2001 The role of vitamin D in prostate cancer. Steroids 66:293-300.
5. Boyle BJ, Zhao XY, Cohen P, Feldman D 2001 Insulin-like growth factor binding protein-3 mediates 1 alpha,25-dihydroxyvitamin d(3) growth inhibition in the LNCaP prostate cancer cell line through p21/WAF1. J Urol 165:1319-24
6. Pollak M 2001 Insulin-like growth factors and prostate cancer. Epidemiol. Rev. 23:59-66
7. Rajah R, Valentinis B, Cohen P 1997 Insulin-like growth factor (IGF)-binding protein-3 induces apoptosis and mediates the effects of transforming growth factor-beta1 on programmed cell death through a p53- and IGF-independent mechanism. J Biol Chem 272:12181-8
8. Pollak M, Beamer W, Zhang JC 1998 Insulin-like growth factors and prostate cancer. Cancer Metastasis Rev 17:383-90.
9. Grimberg A, Cohen P 2000 Role of insulin-like growth factors and their binding proteins in growth control and carcinogenesis. J Cell Physiol 183:1-9.

10. Chan JM, Stampfer MJ, Ma J, Gann P, Gaziano JM, Pollak M, Giovannucci E 2002 Insulin-like growth factor -I (IGF-I) and IGF binding protein -3 as predictors of advanced-stage prostate cancer. J. Natl. Cancer Inst. 94:1099-1106
11. Feldman D, Malloy PJ, Gross C 2001 Vitamin D: biology, action and clinical implications. In: Marcus R, Feldman D, Kelsey J (eds) Osteoporosis. Academic Press, San Diego, vol 1:257-303
12. Haussler MR, Whitfield GK, Haussler CA, Hsieh JC, Thompson PD, Selznick SH, Dominguez CE, Jurutka PW 1998 The nuclear vitamin D receptor: biological and molecular regulatory properties revealed. J Bone Miner Res 13:325-49
13. Liu M, Lee MH, Cohen M, Bommakanti M, Freedman LP 1996 Transcriptional activation of the Cdk inhibitor p21 by vitamin D3 leads to the induced differentiation of the myelomonocytic cell line U937. Genes Dev 10:142-53

0888-8809/04/$15.00/0
Printed in U.S.A.

Molecular Endocrinology 18(5):1109–1119

doi: 10.1210/me.2003-0344

Identification of a Functional Vitamin D Response Element in the Human Insulin-Like Growth Factor Binding Protein-3 Promoter

LIHONG PENG, PETER J. MALLOY, AND DAVID FELDMAN

Department of Medicine, Stanford University School of Medicine, Stanford, California 94305

1,25-Dihydroxyvitamin D_3 [1,25-$(OH)_2D_3$] plays a critical role in maintaining calcium and phosphate homeostasis and bone formation but also exhibits antiproliferative activity on many cancer cells, including prostate cancer. We have shown that the antiproliferative actions of 1,25-$(OH)_2D_3$ in the LNCaP human prostate cancer cell line are mediated in part by induction of IGF binding protein-3 (IGFBP-3). The purpose of this study was to determine the molecular mechanism involved in 1,25-$(OH)_2D_3$ regulation of IGFBP-3 expression and to identify the putative vitamin D response element (VDRE) in the IGFBP-3 promoter. We cloned approximately 6 kb of the IGFBP-3 promoter sequence and demonstrated its responsiveness to 1,25-$(OH)_2D_3$ in transactivation assays. Computer analysis identified a putative VDRE between −3296/−3282 containing the direct repeat motif GGTTCA ccg GGTGCA that is 92% identical with the rat 24-hydroxylase distal VDRE. In EMSAs, the vitamin D receptor (VDR) showed strong binding to the putative IGFBP-3 VDRE in the presence of 1,25-$(OH)_2D_3$. Supershift assays confirmed the presence of VDR in the IGFBP-3 VDRE complex. Chromatin immunoprecipitation assay demonstrated that 1,25-$(OH)_2D_3$ recruited the VDR/retinoid X receptor heterodimer to the VDRE site in the natural IGFBP-3 promoter in intact cells. In transactivation assays, the putative VDRE coupled to a heterologous simian virus 40 promoter construct was induced 2-fold by 1,25-$(OH)_2D_3$. Mutations in the VDRE resulted in a loss of inducibility confirming the critical hexameric sequence. In conclusion, we have identified a functional VDRE in the distal region of the human IGFBP-3 promoter. The induction of IGFBP-3 by 1,25-$(OH)_2D_3$ appears to be directly mediated via VDR interaction with this VDRE. (*Molecular Endocrinology* 18: 1109–1119, 2004)

THE CALCIOTROPIC HORMONE vitamin D, through its biologically active metabolite 1,25-dihydroxyvitamin D_3 [1,25-$(OH)_2D_3$], plays an important role in maintaining calcium and phosphate homeostasis and bone formation (1). In addition, recent evidence has revealed that 1,25-$(OH)_2D_3$ exhibits antiproliferative and differentiation-inducing effects in a variety of cancer cells including prostate cancer (PCa) (2–7). A number of investigations have examined the mechanism of the anticancer action of 1,25-$(OH)_2D_3$ in human PCa cells. Several mechanisms for the anticancer effects of 1,25-$(OH)_2D_3$ have been proposed including G1/G0 cell cycle arrest (4, 8), stimulation of apoptosis by down-regulating the oncogenes *bcl-2* and c-*myc* (9, 10), increase in cyclin-dependent kinase inhibitory protein p21/WAF1 (11, 12), and induction of IGF binding protein-3 (IGFBP-3), which has been shown to inhibit cell growth and stimulate apoptosis (13–15). Our recent studies demonstrate that induction of IGFBP-3 by 1,25-$(OH)_2D_3$ in LNCaP cells is essential for the growth inhibitory action of 1,25-$(OH)_2D_3$ (16). Both immunoneutralization of IGFBP-3 with specific antibodies and antisense treatment that prevents IGFBP-3 synthesis, abolish the growth inhibitory actions of 1,25-$(OH)_2D_3$ (16). Furthermore, IGFBP-3 alone induces p21/WAF1 and IGFBP-3 antisense treatment prevents 1,25-$(OH)_2D_3$ induction of p21/WAF1 and abrogates its antiproliferative activity (16). We have shown that 1,25-$(OH)_2D_3$ increases IGFBP-3 expression and protein levels in LNCaP cells (16). We also showed using cDNA microarrays that the expression of IGFBP-3 increases after 1,25-$(OH)_2D_3$ treatment of LNCaP cells (17). Furthermore, epidemiological studies indicate that low IGF-I and high IGFBP-3 levels in the circulation lower the risk of PCa, providing additional support for a linkage between the IGF axis and 1,25-$(OH)_2D_3$ in PCa (18–24).

IGFBP-3 is a member of the IGFBP family that binds the potent mitogen IGF-I with high affinity and specificity. IGFBPs serve to extend half-life as well as transport and modulate the biological actions of IGFs on target cells. IGFBP-3 is the most abundant circulating IGFBP binding more than 75% of serum IGFs (25). In addition to regulating IGF action and bioavailability, IGFBP-3 also mediates IGF-independent actions, including inhibition of cell growth and induction of apo-

Abbreviations: ChIP, Chromatin immunoprecipitation; DTT, dithiothreitol; FBS, fetal bovine serum; IGFBP, IGF binding protein; 1,25-$(OH)_2D_3$, 1,25-dihydroxyvitamin D_3; PCa, prostate cancer; RXR, retinoid X receptor; SV40, simian virus 40; VDR, vitamin D receptor; VDRE, vitamin D response element.

***Molecular Endocrinology* is published monthly by The Endocrine Society (http://www.endo-society.org), the foremost professional society serving the endocrine community.**

ptosis (13, 26, 27). Several mechanisms of IGF-independent actions of IGFBP-3 have been revealed. These include IGFBP-3 binding to TGFβ type V receptor (28), nuclear translocation via the importin β-subunit (29), and direct interaction with the nuclear receptor retinoid X receptor α (RXRα) (30, 31). IGFBP-3 expression is regulated by specific growth promoters and inhibitors including TGFβ (32, 33), retinoic acid (33), vitamin D (14, 16), TNFα (34), the histone deacetylase inhibitors trichostatin A and sodium butyrate (35), as well as p53 (14, 34, 36–38). However, limited information is known regarding functional response elements within the human IGFBP-3 promoter. Only p53 has been shown to up-regulate IGFBP-3 synthesis *in vitro* via direct protein/gene interaction (37).

The purpose of this study was to investigate the molecular mechanism of IGFBP-3 regulation by 1,25-$(OH)_2D_3$ in PCa. The actions of 1,25-$(OH)_2D_3$ are mediated by the vitamin D receptor (VDR), a member of the steroid hormone receptor superfamily. The VDR heterodimerizes with RXR and modulates gene expression in a ligand-dependent manner via specific vitamin D response elements (VDREs) in target gene promoters (39–41). As discussed above, we have previously shown that the antiproliferative actions of 1,25-$(OH)_2D_3$ are due in part to up-regulation of IGFBP-3 (16). In this study, we examined the molecular mechanism of 1,25-$(OH)_2D_3$ action on the IGFBP-3 promoter in LNCaP cells and identified and characterized a functional VDRE in this promoter.

RESULTS

Induction of IGFBP-3 mRNA by 1,25-$(OH)_2D_3$ in LNCaP Cells

We have previously shown that treatment of LNCaP cells with 1–1000 nM of 1,25-$(OH)_2D_3$ for 48 h caused a 1.3- to 2.9-fold increase of IGFBP-3 at both message and protein levels (16). To further elucidate the mechanism for 1,25-$(OH)_2D_3$ induction of IGFBP-3, we performed a time course of IGFBP-3 mRNA expression in LNCaP cells treated with 10 nM 1,25-$(OH)_2D_3$. As shown in Fig. 1, at 6 h IGFBP-3 mRNA is induced 2.7-fold in the 1,25-$(OH)_2D_3$-treated cells. At 12 h, the IGFBP-3 mRNA peaks and remains elevated after 48 h, which is consistent with our previous report (16). The IGFBP-3 protein level is increased approximately 3-fold after 48 h achieving concentrations of 3–6 ng/ml in the conditioned medium of 1,25-$(OH)_2D_3$-treated LNCaP cells (16). These results suggest that 1,25-$(OH)_2D_3$ may directly regulate the transcription of IGFBP-3 in LNCaP cells. Although growth inhibition by exogenously added IGFBP-3 appears to require 10–100 ng/ml of the protein, the intracrine as well as paracrine effects of endogenously synthesized IGFBP-3 induced by 1,25-$(OH)_2D_3$ appear to be sufficient to cause growth inhibition (16).

Induction of the IGFBP-3 Promoter Activity by 1,25-$(OH)_2D_3$ in LNCaP Cells

To determine whether 1,25-$(OH)_2D_3$ is involved in the transcriptional regulation of the IGFBP-3 gene in LNCaP cells, we cloned a PCR fragment containing approximately 1.9 kb of the published IGFBP-3 promoter sequence (−1901 to +55) (42) into the promoterless luciferase reporter vector, pGL3-basic. We then cotransfected this construct with a VDR expression vector (pSG5-VDR) into LNCaP and HeLa cells. As shown in Fig. 2, the 1.9-kb fragment showed no stimulation by 1,25-$(OH)_2D_3$ in either cell line. We then used the published sequence to search the GenBank database to obtain more 5′ flanking sequence. Based on our search, we generated further upstream sequence of the IGFBP-3 promoter by PCR. A DNA fragment from −1901 to −3595 was ligated to the

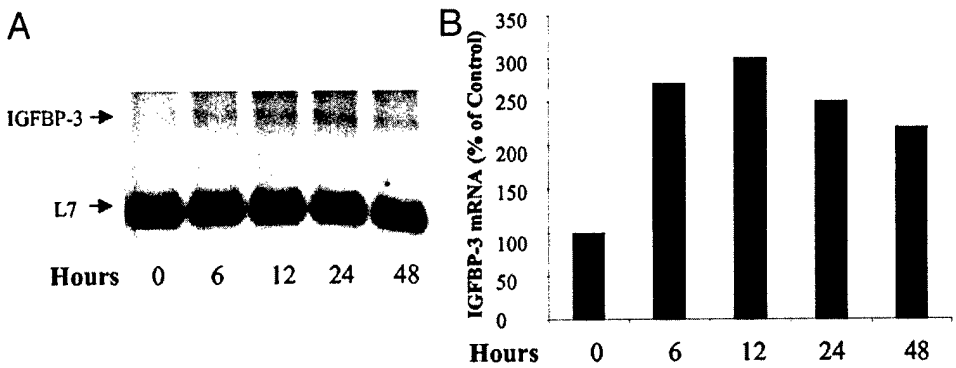

Fig. 1. Time Course of 1,25-$(OH)_2D_3$ Up-Regulation of IGFBP-3 mRNA in LNCaP Cells

A, Confluent LNCaP cells were treated with vehicle or 10 nM 1,25-$(OH)_2D_3$ in 1% FBS-RPMI medium for 0, 6, 12, 24, and 48 h. RNA was collected and transferred to membranes by Northern blotting. The blot was hybridized with ^{32}P-labeled IGFBP-3 and L7 probes. Northern blot analysis of time course shows up-regulation of IGFBP-3 mRNA. Ribosomal protein L7 serves as a control for RNA loading. B, Quantitation of Northern blot was performed using densitometric analysis with each value expressed as percent of vehicle-treated control.

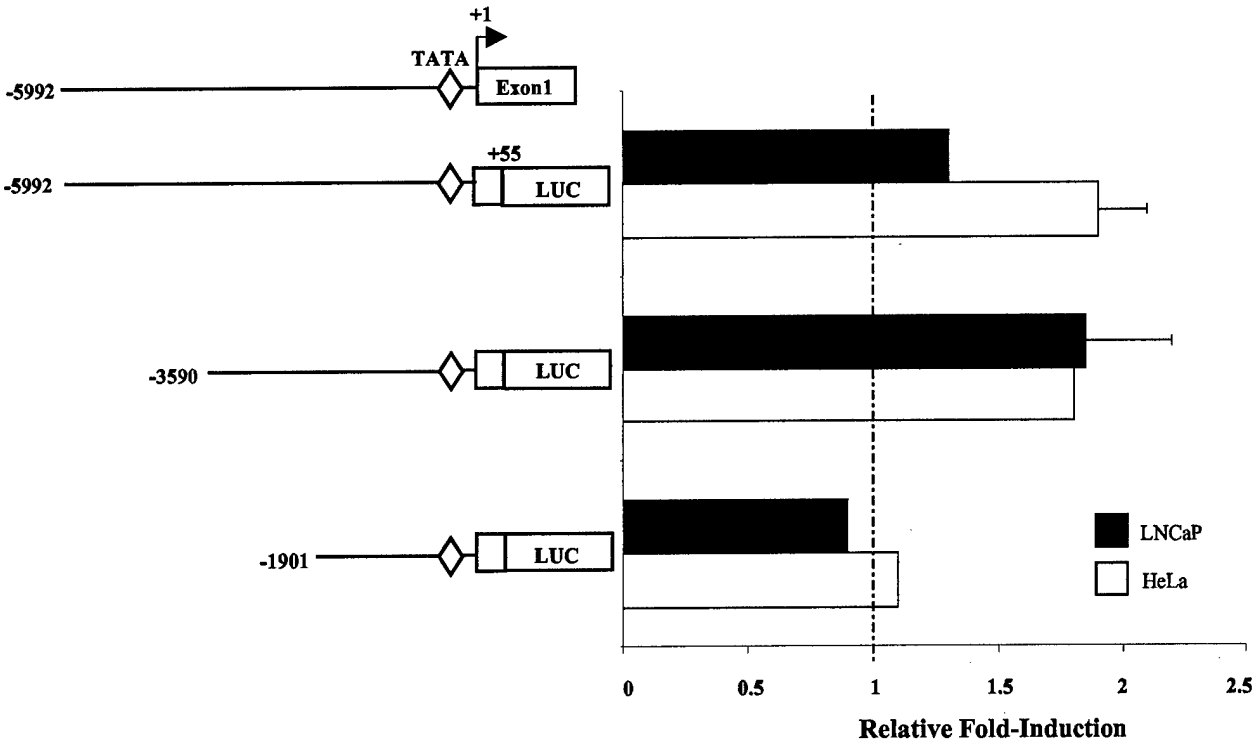

Fig. 2. Transcriptional Activation of the Human IGFBP-3 Promoter by 1,25-$(OH)_2D_3$

The IGFBP-3 promoter (1.9 kb) and deletions thereof were cloned into the pGL3-Basic reporter vector as indicated on the *left*. Numbers are in reference to the transcription start site that is at +1. These constructs were transiently cotransfected with pSG5-VDR expression vector into LNCaP and HeLa cells. The cells were treated with vehicle or 10 nM 1,25-$(OH)_2D_3$ for 16–18 h. A *Renilla* luciferase expression vector was used to control for transfection efficiency. The activity of each construct was expressed as 1,25-$(OH)_2D_3$ treatment *vs.* control that is set as 1. Each value represents the mean of two independent transfections, each performed in triplicate.

−1901 construct, generating a promoter sequence from −3595 to +55. In transactivation assays, this promoter sequence showed approximately 2-fold induction by 1,25-$(OH)_2D_3$ in both LNCaP and HeLa cells (Fig. 2). No further increase in 1,25-$(OH)_2D_3$ transactivation was observed when sequences up to −5992 were tested. These results suggest that a putative VDRE is present in the region from −3595 to −1901 of the IGFBP-3 promoter.

Identification of a Functional VDRE in the Distal Promoter of the IGFBP-3 Gene

To determine whether the sequence between −3590 and −1901 can act as an enhancer element, the sequence from −3590 to −1753 was cloned 5′ of the heterologous simian virus 40 (SV40) promoter in the pGL3-promoter vector. LNCaP and HeLa cells were cotransfected with this chimeric construct and pSG5-VDR and then treated with 10 nM 1,25-$(OH)_2D_3$. As shown in Fig. 3A, the sequence from −3590 to −1753 showed an increase in SV40 promoter activity of about 1.8-fold in LNCaP and 2.5-fold in HeLa cells, demonstrating 1,25-$(OH)_2D_3$ responsiveness by this 1.8-kb fragment.

To further define the VDRE within this 1.8-kb fragment of the IGFBP-3 promoter, deletions were generated, cloned into the pGL3-promoter vector and then transfected into HeLa cells. As shown in Fig. 3B, removal of the 3′ sequence from −1753 to −2474 did not change the enhancer activity. Further deletions from −2950 to −2474 and from −3205 to −2950 displayed similar enhancer activity. The data suggest that a VDRE is located in the 386-bp fragment between −3590 and −3205. Additional deletions within this fragment were made to characterize the minimal enhancer sequence (Fig. 3B). When the 5′ sequence was further deleted from −3590 to −3410, the activity remained the same as the −3590/−3205 construct. Further 3′ deletion from −3410 to −3205, however, resulted in complete loss of the enhancer activity. The data suggest that the VDRE is located within this 206-bp fragment between −3410 and −3205.

The VDREs are generally composed of two direct repeats of six bases separated by a three-nucleotide spacer referred to as a DR3 motif. Computer analysis of the 206-bp fragment identified a potential VDRE (GGTTCA ccg GGTGCA) located between −3296 and −3282. We refer to this 15-bp sequence as BP3-VDRE. This sequence contains two hexameric core

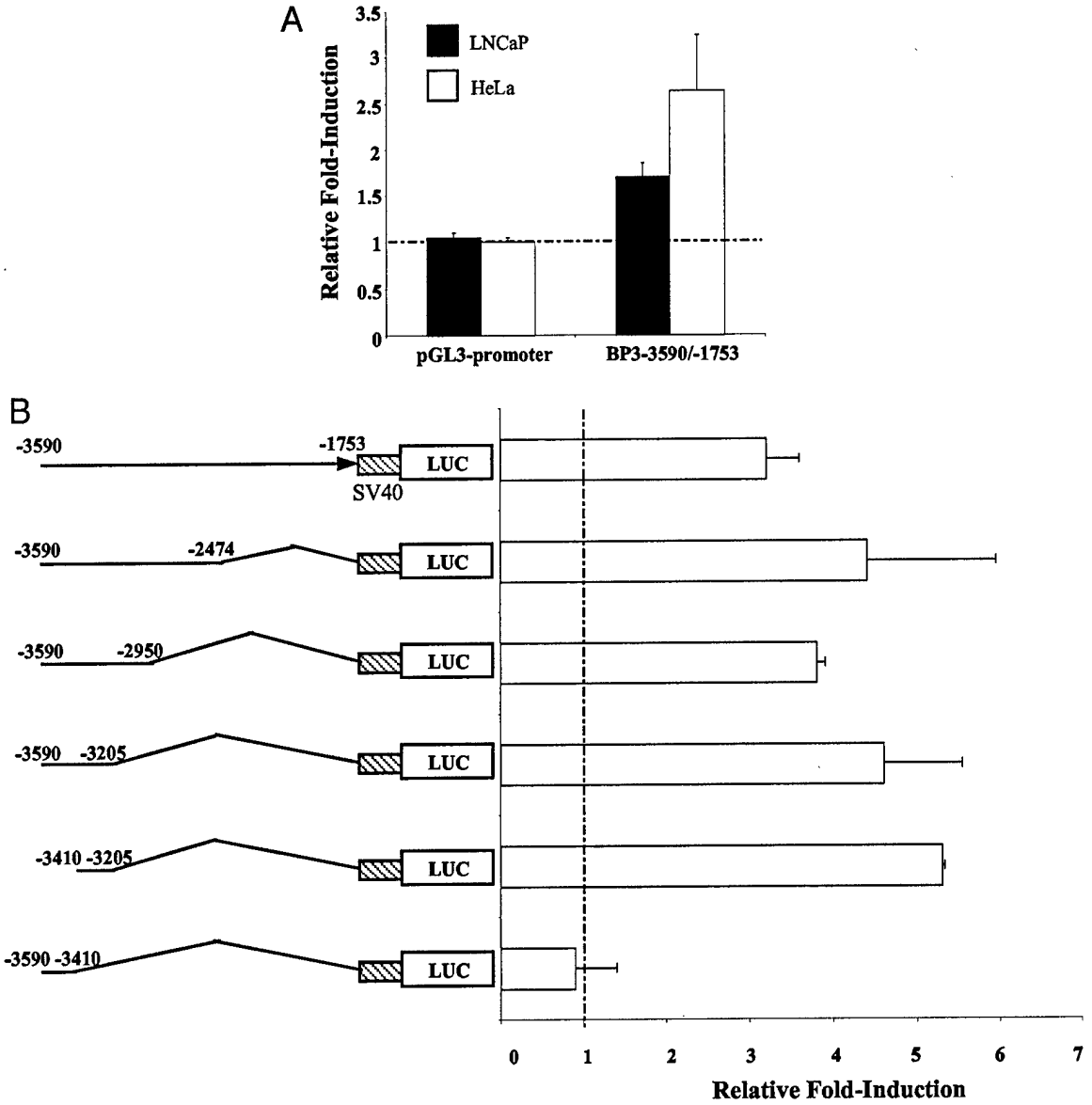

Fig. 3. Localization of the VDRE Enhancer to a Short Region of the Human IGFBP-3 Promoter

A, A 1.85-kb fragment encompassing nucleotides −3590 and −1901 of the IGFBP-3 promoter was cloned into the SV40 promoter-driven luciferase reporter vector pGL3-promoter. The reporter construct was transfected into LNCaP and HeLa cells and then treated with 10 nM 1,25-$(OH)_2D_3$. The activity of the construct was expressed as fold increase over control. Data are representative of three independent experiments, mean ± SE. B, Deletions both 5′ and 3′ made within the sequence between −3590 and −1753 (as illustrated on the *left*) were cloned into the pGL3-promoter vector and transfected into HeLa cells. The activity of each construct is expressed as fold induction over control. Each value represents the average of two experiments, each performed in triplicate.

sites separated by three nucleotides resembling a DR3 motif. As shown in Table 1, the BP3-VDRE is 92% identical with the distal VDRE of the rat 24-hydroxylase promoter located at −259 (designated r24-OH-distal VDRE) and 87% identical with the VDRE consensus sequence (43).

Confirmation of VDRE Properties by EMSA and Chromatin Immunoprecipitation (ChIP) Assay

We used EMSA to determine whether the VDR can bind to the putative IGFBP-3 VDRE sequence. Double-stranded BP3-VDRE and r24-OH distal VDRE oligonucleotides were incubated with crude cell extracts from COS-7 cells transfected with pSG5 or pSG5-VDR vectors. A strong specific DNA-protein complex with the VDR-transfected cell extracts was observed both with probe BP3-VDRE (Fig. 4B, lane 4) and with probe r24-OHdistal VDRE (data not shown). This binding activity was highly induced by 10 nM of 1,25-$(OH)_2D_3$ (Fig. 4B, lane 5). A complex with identical mobility to the VDR-transfected cell extracts was also observed with the

Table 1. Comparison of VDRE in the IGFBP-3 Promoter to Known VDREs

Source	Sequence[a]	Identity (%)	Position
Consensus VDRE[b] (37)	**PuGGTCA NNG PuGTTCA**	100	
Human osteopontin (52)	**GGGTC**G TAT **GGTTCA**	87	−1892/−1878
Rat 24-OHase-distal (41)	**GGTTCA** GC**G GGTGC**G	80	−259/−245
Human 24-OHase (43)	**AGTTCA** CC**G GGT**GTG	73	−293/−273
Human IGFBP-3[c]	**GGTTCA** CC**G GGTGCA**	87	−3296/−3282
Mouse IGFBP-3[d]	**TGGTTA** GAA **GGTGCA**	73	−2505/−2490

[a] Nucleotides identical to the VDRE consensus sequence are in *bold.*
[b] Consensus VDRE determined by binding of VDR/RXR heterodimers to randomly selected high affinity VDRE. Pu = A or G.
[c] GenBank accession no. AC091524.
[d] GenBank accession no. AL607124.

empty vector-transfected cell extracts (Fig. 4B, lane 2); however, it was not induced by 1,25-$(OH)_2D_3$ (Fig. 4B, lane 3). When a 200-fold molar excess of unlabeled oligonucleotide, either BP3-VDRE or r24-OHdistal VDRE, was added, the signal was diminished (Fig. 4B, lanes 6 and 7). In contrast, when an unlabeled oligonucleotide containing mutations in either the 5′ (BP3-VDREm1) or the 3′ (BP3-VDREm2) hexamic sequence (Fig. 4A) was added, the DNA-binding was no longer competed (Fig. 4B, lanes 8 and 9). These results indicate that the BP3-VDRE sequence may be similar to the r24-OH distal VDRE that binds the nuclear proteins VDR and RXR.

To confirm the presence of VDR and protein in the BP3-VDRE complex, VDR or RXRα antibodies were added for supershift assays. As shown in Fig. 4C, the BP3-VDRE sequence was bound by proteins recognized by VDR or RXRα antibodies, thus producing supershifted complex SS1 (lane 3) or complex SS2 (lane 4), respectively. Both complexes SS1 and SS2 were of similar mobility to that seen with the r24-OHdistal VDRE probe (data not shown).

ChIP assays were performed to further prove that 1,25-$(OH)_2D_3$ was capable of recruiting VDR/RXR to the chromatinized BP3-VDRE in the native IGFBP-3 promoter in the absence of VDR overexpression. LNCaP cells were treated with or without 1,25-$(OH)_2D_3$ and then subjected to ChIP assay. PCR was performed with the purified immunoprecipitated chromatin DNA using the primers designed to amplify the IGFBP-3 promoter sequence encompassing BP3-VDRE. As shown in Fig. 5, with the antibody against VDR (lanes 5 and 6) or RXRα (lanes 7 and 8) added in the immuoprecipitation reaction, an expected size band was produced only in the 1,25-$(OH)_2D_3$-treated cells (lanes 6 and 8), indicating that the BP3-VDRE is the interacting sequence with the VDR/RXR complex. The results further confirm a functional VDRE site in the natural chromatin structure in the intact cells.

Therefore, our EMSA and ChIP assay results strongly indicate that the BP3-VDRE sequence in the human IGFBP-3 promoter is a novel VDR binding element.

Confirmation of Enhancer Activity of the BP3-VDRE by Transactivation

To determine whether the BP3-VDRE sequence acts as an enhancer in a 1,25-$(OH)_2D_3$ inducible fashion, a single copy of this sequence was cloned into the pGL3-promoter expression vector upstream of the heterologous SV40 promoter in both sense and antisense orientations (Fig. 6). LNCaP cells cotransfected with the BP3-VDRE/SV40 promoter chimeric constructs and pSG5-VDR showed approximately 2-fold induction of luciferase activity in the presence of 10 nM 1,25-$(OH)_2D_3$ as compared with the cells without 1,25-$(OH)_2D_3$. This increase occurred whether the BP3-VDRE was in the sense or antisense orientation. The pGL3-promoter empty vector showed no 1,25-$(OH)_2D_3$ induction (data not shown). The mutations (Fig. 4A) in the RXR-binding site (m1) or VDR-binding site (m2) of the BP3-VDRE enhancer, which disrupt VDR/RXR binding in the EMSA study (Fig. 4B), were also introduced into the BP3-VDRE/SV40 promoter hybrid construct. As shown in Fig. 6, both mutants m1 and m2 resulted in loss of 1,25-$(OH)_2D_3$ inducibility, indicating that the two hexameric sequences are required for the enhancer activity of the BP3-VDRE. To reveal whether BP3-VDRE functions in the same manner in both the native promoter and the heterologous SV40 promoter, the same mutations (m1 or m2) were introduced into the −5992/+55 native promoter reporter construct. Neither mutant showed induction by 1,25-$(OH)_2D_3$ that is comparable to the mutated heterologous promoter construct (Fig. 6).

DISCUSSION

Previous studies from our lab have demonstrated that IGFBP-3 is a direct mediator of 1,25-$(OH)_2D_3$ antiproliferative action in LNCaP human PCa cells (16). However, the mechanism by which 1,25-$(OH)_2D_3$ up-regulates IGFBP-3 is unknown. In this study, we identified a functional VDRE (BP3-VDRE) located between −3296 and −3282 upstream of the human IGFBP-3 gene. Thus, 1,25-$(OH)_2D_3$ is able to directly

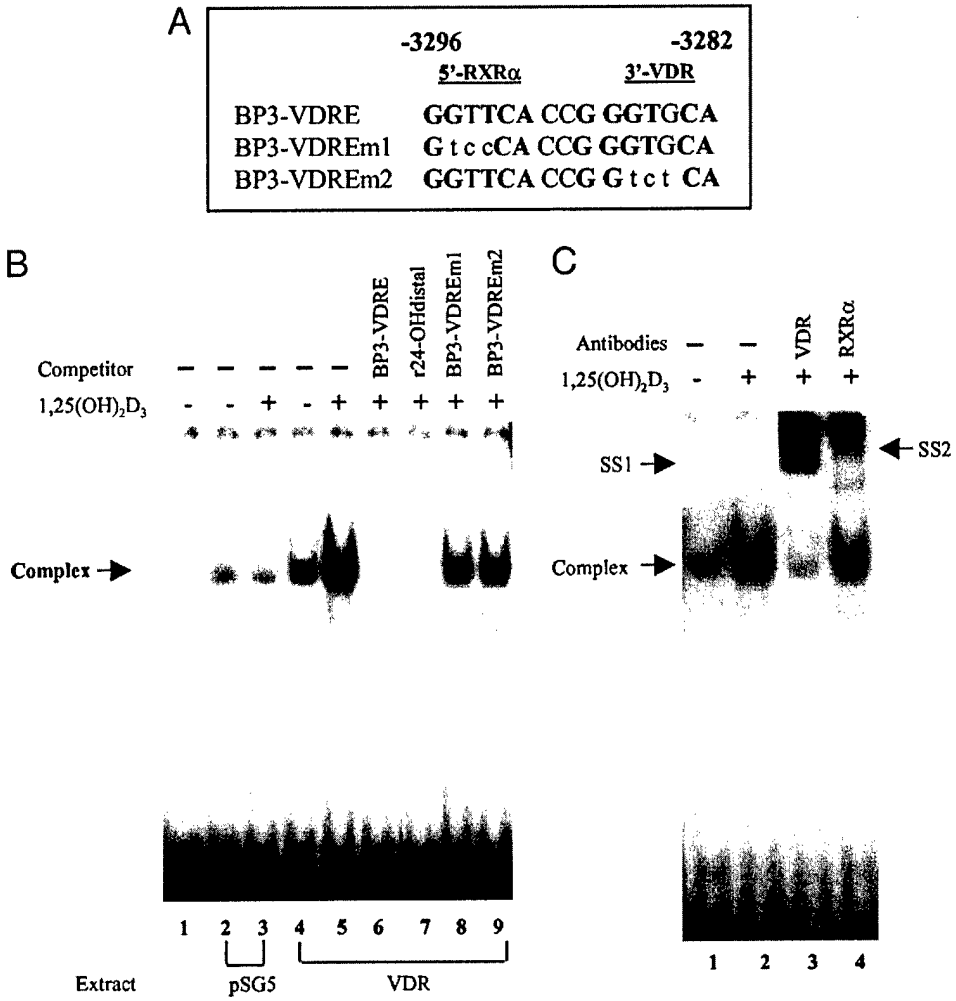

Fig. 4. Specific Binding Activity of VDR to the Putative BP3-VDRE Sequence

A, Nucleotide sequences of wild-type BP3-VDRE or mutated BP3-VDREs containing mutations in the 5′ RXRα binding site (BP3-VDREm1) or in the 3′ VDR binding site (BP3-VDREm2). The consensus nucleotides for VDR/RXR binding are illustrated in *bold* with *lower case letters* representing the mutated nucleotides. B, EMSA. The nucleotides were annealed and end-labeled with [γ-^{32}P]ATP using T_4 polynucleotide kinase. The labeled probe BP3-VDRE was then incubated with 5 μg of cell extracts isolated from transfected COS-7 cells with empty vector pSG5 (lanes 2 and 3) or with VDR expression vector (lanes 4–9) in the absence or presence of 1,25-$(OH)_2D_3$. Lane 1, No cell extract. C, Supershift was performed with specific antisera to VDR or RXRα in the absence or presence of 1,25-$(OH)_2D_3$ yielding supershifted complexes SS1 and SS2, respectively.

activate IGFBP-3 expression at the transcriptional level through binding of the hormone-bound VDR/RXR heterodimer to BP3-VDRE. The presence of a VDRE in the IGFBP-3 promoter is strongly supported by the fact that the BP3-VDRE sequence confers 1,25-$(OH)_2D_3$ responsiveness both in its natural promoter setting and in a heterologous promoter system. Moreover, mutations within the BP3-VDRE abolish 1,25-$(OH)_2D_3$ induction of both heterologous and natural promoters. Also, the specific binding of VDR to this responsive element is demonstrated in gel shift assays and importantly, addition of anti-VDR or anti-RXRα antibodies causes supershift of the BP3-VDRE complex. This BP3-VDRE complex can be competed with unlabeled BP3-VDRE and r24-OH distal VDRE sequences, but not with mutated BP3-VDRE sequences. Furthermore, ChIP assays demonstrate that 1,25-$(OH)_2D_3$ is able to recruit the VDR/RXR heterodimer to the VDRE site in the context of native IGFBP-3 promoter architecture.

The BP3-VDRE shows an 87% identity to the rat 24-hydroxylase distal VDRE (43, 44). The 24-hydroxylase is the most responsive known primary 1,25-$(OH)_2D_3$ target gene in mammals (43, 45). The rat 24-hydroxylase promoters has two VDREs, a distal VDRE located at −259, and a proximal VDRE at −152 from the transcription start site (Table 1) (43). These two sites located in close vicinity to each other and to the transcription start site synergistically contribute to the strong responsiveness of the gene to 1,25-$(OH)_2D_3$ treatment. When fused to the thymidine kinase promoter, the 24-OHase distal VDRE results in a 2.5-fold

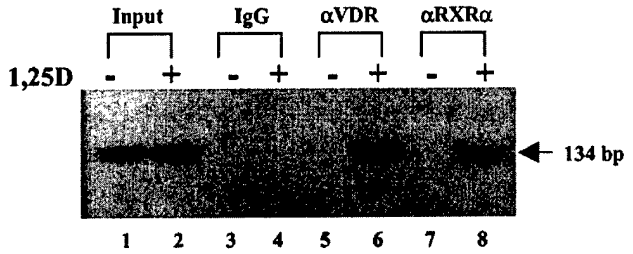

Fig. 5. ChIP Assay Demonstrating that VDR and RXRα Are Recruited to the IGFBP-3 Promoter by 1,25-$(OH)_2D_3$ in LNCaP Cells

LNCaP cells were plated at 3×10^6 cells per 10-cm dish and treated with (+) or without (−) 10 nM of 1,25-$(OH)_2D_3$. After 18 h, the cells were subjected to ChIP assay as described in *Materials and Methods*. After the immunoprecipitation, the samples were amplified by PCR using primers designed to amplify a 134-bp fragment of the IGFBP-3 promoter from −3340 to −3207 encompassing the BP3-VDRE. Lanes 1 and 2, Input DNA; lanes 3 and 4, mouse IgG; lanes 5 and 6, anti-VDR; lanes 7 and 8, anti-RXRα.

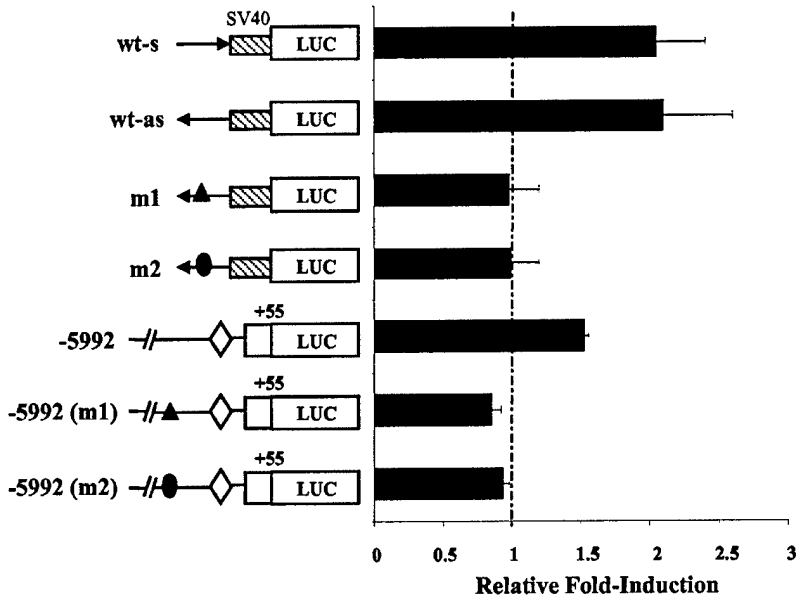

Fig. 6. The BP3-VDRE Is a Functional VDRE

A single copy of wild-type BP3-VDRE sequence in either the sense (wt-s) or antisense orientation (wt-as), as well as mutated BP3-VDRE (m1 or m2) in the antisense direction, was cloned into the pGL3-promoter reporter vector. The m1 and m2 oligonucleotides are the same as used in the EMSA (Fig. 4A). The m1 oligonucleotide has a mutation in the RXRα binding site (▲), whereas the m2 contains a mutation in the VDR binding site (●). The same mutations were also introduced into the −5992/+55 pGL3-Basic reporter construct. Either the heterologous or the natural promoter constructs were cotransfected with pSG5-VDR into LNCaP cells and treated with ethanol or 10 nM 1,25-$(OH)_2D_3$ for 16–18 h. The activity of each construct is expressed as fold induction over control. Data are representative of three independent experiments, each performed in triplicate.

induction by 1,25-$(OH)_2D_3$ (44) similar to the BP3-VDRE, which confers about 2-fold induction by 1,25-$(OH)_2D_3$. We also observed that two copies of the BP3-VDRE sequence in the heterologous promoter doubled the enhancer activity relative to a single copy of BP3-VDRE indicating a gene dosage effect (data not shown). However, the transactivation assays reported here were amplified only to a limited degree despite overexpression of VDR. In the absence of overexpressed VDR, 1,25-$(OH)_2D_3$ induction of the BP3-VDRE was only about 1.2-fold (data not shown). However, cDNA microarray and Northern blot analyses showed a remarkable induction of IGFBP-3 message in the absence of overexpressed VDR when LNCaP cells were treated with 1,25-$(OH)_2D_3$ (16, 17). Indeed, the best induction by 1,25-$(OH)_2D_3$ occurred when the BP3-VDRE was in its natural setting. It is possible that the low level of BP3-VDRE transactivation *in vitro* results from its distant location to the transcriptional machinery (46). In its natural promoter context, the VDRE's response to 1,25-$(OH)_2D_3$ may be enhanced through interaction with additional flanking partner proteins. In addition, the functionality of a 1,25-$(OH)_2D_3$ responding gene, such as the 24-OHase gene, may depend upon the potential synergistic action of two or more VDREs (45). Although up to 6000 bp of promoter sequence has been examined in this study, the presence of additional VDRE(s) cannot be excluded in the IGFBP-3 gene.

VDREs have been identified in a number of other 1,25-$(OH)_2D_3$ target genes including osteocalcin and osteopontin (47–54), β_3 integrin (55), 24-hydroxylase (43, 44, 56, 57), and calbindin-D_{28k} (58). All of these VDRE sites are located within the first 800 bp of promoter sequence upstream of the transcription start site. The IGFBP-3 VDRE, on the other hand, is uniquely located in the distal promoter region over 3 kb upstream from the transcription start site. In addition, computer analysis of the mouse IGFBP-3 promoter sequence predicts a putative VDRE site whose core binding sequence is 75% homologous to the human BP3-VDRE that we identified. This putative mouse IGFBP-3 VDRE is located at −2505 from the transcription start site (Table 1); however, its functionality remains to be tested.

We and others (11, 16) have shown that 1,25-$(OH)_2D_3$ up-regulates p21 a major regulator of the cell cycle. However, there is controversy about whether the action of 1,25-$(OH)_2D_3$ on p21 is a direct or an indirect effect (16, 59). Although Liu *et al.* (11) demonstrated that 1,25-$(OH)_2D_3$ directly acted on p21 gene expression through a functional VDRE in the promoter of the p21 gene in U937 leukemia cells, we could not demonstrate a direct effect in LNCaP cells. Indeed, we found that p21 up-regulation by 1,25-$(OH)_2D_3$ can be inhibited by immunoneutralization of IGFBP-3, which suggests that p21 induction is mediated by IGFBP-3 and indirectly by 1,25-$(OH)_2D_3$ (16). This lack of a direct effect is supported by Eelen *et al.*'s recent report (59) in the mouse bone cells and keratinocytes. However, it is possible that a hormone-responsive element may be active only in an appropriate cellular environment due to cell specificity.

Our findings provide significant insight into the molecular regulation of IGFBP-3 by 1,25-$(OH)_2D_3$. Together with our previous data (16), we demonstrate that 1,25-$(OH)_2D_3$ directly increases IGFBP-3 expression through binding to the BP3-VDRE site in the IGFBP-3 promoter in LNCaP cells. IGFBP-3 may then act via paracrine or intracrine pathways to activate pathways including activation of p21/WAF1 causing cell cycle arrest or cell death through induction of apoptosis (30, 60). In conclusion, our study provides strong evidence showing that 1,25-$(OH)_2D_3$ directly regulates IGFBP-3 via a VDRE located approximately 3 kb upstream in the IGFBP-3 promoter. These findings provide additional insight into 1,25-$(OH)_2D_3$ regulation of target genes as well as adding further data on the variable nature and location of VDREs.

MATERIALS AND METHODS

Cell Cultures

Human cervical adenocarcinoma cells, HeLa (ATCC CCL-2) and monkey kidney fibroblast cells, COS-7 (ATCC CRL-1651), were cultured in DMEM supplemented with 10% fetal bovine serum (FBS) (Life Technologies, Inc., Rockville, MD). The human prostate carcinoma cell line, LNCaP (ATCC CRL-1740), was grown in RPMI 1640 medium containing 5% FBS. All cells were maintained at 37 C in a humidified atmosphere with 5% CO_2.

Northern Blot Analysis of IGFBP-3 mRNA

LNCaP cells were treated with 10 nM 1,25-$(OH)_2D_3$ or ethanol control in 1% FBS medium. At specific time intervals, the cells were collected and total RNA extracted using TRIZOL reagent (Invitrogen, Carlsbad, CA). Northern blots were performed as previously described (61). A 200-bp fragment representing exon 2 of the human IGFBP-3 gene was labeled with [α-^{32}P]deoxy-CTP using the Rediprime DNA labeling kit (Amersham, Piscataway, NJ). The ribosomal protein gene L7 was used as a control to normalize RNA loading and transfer efficiency.

Construction of Plasmids for Promoter Analysis

The 1.9 kb of the published IGFBP-3 promoter sequence (42) was amplified by PCR and cloned into the promoterless luciferase reporter vector pGL3-basic (Promega, Madison, WI). Additional 5′ flanking sequence was determined from the GenBank database (AC091524) using sequence homology searches with the 1.9-kb promoter sequence. Three fragments (A, −1901/+55; B, −3590/−1753; and C, −5992/−3590) were generated by PCR from human genomic DNA (CLONTECH, Palo Alto, CA) using primers containing restriction enzyme sites. The sequences of these primers were shown as follows: fragment A—upper, 5′-GGAATCCAGGCAGGAAGCGGCTGAT-3′; lower, 5′-AGACCTGGGACCTCAAGAATTGCAT-3′; fragment B—upper, 5′-AACTCTGAGGAGCCCCTGTCT-3′;lower,5′-TAGTATCTGCGTTGACACCCA-3′; fragment C—upper, 5′-GGGGTACCAAATGTGCAAGAGTAGCACTAC-3′; lower, 5′-CAGTGGTACCTGTGGCAGTGGAAAT-3′. PCR was performed using the following conditions: 95 C for 5 min, then 35 cycles of 94 C for 1 min, 60 C for 1 min, and 72 C for 2 min with a final step of 72 C for 10 min. PCR products were TOPO-cloned into the pCR2.1 TA-TOPO cloning vector (Invitrogen). The nucleotide sequence of the PCR fragments was confirmed by sequencing. The promoter fragments were then directionally cloned into the pGL3-basic vector. Fragment A (1.95 kb) was cloned into the pGL3-basic at the *Kpn*I and *Hin*dIII sites (pGL3-A), fragment B (1.85 kb) to the *Kpn*I-*Hin*dII sites of pGL3-A (pGL3-B), and fragment C (2.4 kb) at the *Kpn*I sites of pGL3-B (pGL3-C). Plasmid DNA was prepared using plasmid purification kits (QIAGEN, Valencia, CA).

Heterologous Constructs for Enhancer Analysis

The 1.85-kb *Kpn*I-*Hin*dII fragment (−3590/−1753) from plasmid pGL3-B was cloned into the *Kpn*I/*Sma*I sites of pGL3-promoter vector, a heterologous SV40 promoter-driven luciferase reporter (Promega). Further deletions within the −3590/−1753 fragment, including sequences −3590/−2474, −3590/−2950, −3590/−3205, −3590/−3410, and −3410/−3205, were made using internal restriction sites and then cloned into pGL3-promoter at the *Sma*I site. A pair of oligonucleotides 5′-CGCGTTATAAATGCACCCGGTGAACCTCTCTGA-3′ and 5′-CGCGTCAGAGAGGTTCACCGGGTGCATTTATAA-3′, located between −3303 and −3276 enclosing the putative VDRE site were synthesized (Operon, Alameda, CA) containing an *Mlu*I overhang on the 5′ end. These oligonucleotides were annealed and ligated to the *Mlu*I site of the pGL3-promoter vector. The orientation of each insert in the heterologous construct was verified by sequencing.

Mutagenesis in the BP3-VDRE Sequence in the Natural and Heterologous Promoters

Mutations in the potential RXR (m1) or VDR (m2) binding site in the BP3-VDRE sequence were introduced into the −5992/+55/pGL3-Basic reporter construct by the GeneEditor *in vitro* Site-Directed Mutagenesis System (Promega) following the manufacturer's instructions. Two pairs of oligonucleotides containing same mutations m1 or m2 in the BP3-VDRE sequence with *Mlu*I site overhangs were synthesized and directly cloned to the pGL3-promoter vector. Positive clones were identified by sequencing.

DNA Transfections and Luciferase Assay

LNCaP cells were plated at a density of 5×10^5 cells/35-mm in six-well plates the day before transfection. At approximately 75% confluence, the cells were transfected with 1 μg DNA using 2 μl of TransIT-Insecta transfection reagent per well (Mirus, Madison, WI). HeLa cells (7.5×10^4/20-mm in 12-well plates) were transfected at approximately 70% confluence using PolyFect transfection reagent (QIAGEN). Ten nanograms of the *Renilla* luciferase plasmid pRL-null (Promega) were included in each transfection to control for the transfection efficiency. After 20 h, the cells were treated with 10 nM 1,25-$(OH)_2D_3$ or ethanol for 16–18 h. The cells were lysed using Passive Lysis Buffer (Promega). Luciferase activity was determined using the Dual Luciferase Assay System (Promega) that was normalized to the *Renilla* luciferase activity. The induction of each construct's luciferase activity by 1,25-$(OH)_2D_3$ was expressed as fold induction over ethanol control.

Expression of VDR in COS-7 Cells

COS-7 cells were grown to approximately 80% confluence in 10-cm tissue culture flasks and transfected with 2 μg of empty vector pSG5 or VDR expression plasmid pSG5-VDR using the PolyFect agent as described previously (62). After a 48-h transfection, the cells were collected, rinsed with PBS, and resuspended in M-PER mammalian cell extraction buffer (Pierce Chemical Co., Rockford, IL) containing 300 mM KCl, 5 mM dithiothreitol (DTT) and a protease inhibitor tablet (1 tablet/50 ml) (Roche Molecular Biochemicals, Indianapolis, IN). After 10 min incubation at ambient temperature, the suspension was centrifuged at 12,000 × *g* for 10 min at 4 C. The cell extracts were aliquoted and stored at −80 C.

EMSA

Double-stranded oligonucleotide BP3-VDRE (5′-AAATGCACC CGGTGAACCTCTC-3′) was radiolabeled with [γ-^{32}P]ATP using T_4 polynucleotide kinase. Unincorporated radionucleotides were separated using the Nucleotide Removal Kit (QIAGEN). EMSAs were performed in 20 μl of binding reaction containing 4 mM HEPES (pH 7.9), 150 mM KCl, 1.5 mM $MgCl_2$, 1 mM DTT, 1 mM EGTA, 10% glycerol, 2 μg poly (deoxyinosine:deoxycytosine), 5 μg cellular extract, and 0.1–0.4 ng radiolabeled probes (50,000 cpm/reaction) as described previously (63, 64). Samples were incubated with 10 nM 1,25-$(OH)_2D_3$ or ethanol for 15–20 min at ambient temperature (62). For competition assays, a 500-fold molar excess of unlabeled oligonucleotides was added to the binding reaction mixture for 20 min before the addition of the probe. For supershift assays, 2 μg of RXRα or VDR polyclonal antibodies (Santa Cruz Biotechnology, Santa Cruz, CA) were added to the binding reaction mixture 40 min before the addition of the probe. After an additional 20 min incubation, the bound DNA-protein complexes were resolved by electrophoresis on 5% nondenaturing polyacrylamide gels in 0.5× Tris-borate-EDTA buffer containing 45 mM Tris (pH 8.0), 45 mM borate, and 1 mM EDTA at 170 V constant voltages for 1.5 h. The gels were dried and exposed to x-ray film at −80 C.

ChIP

ChIP assay was carried out using the Upstate Biotechnology (Charlottesville, VA) ChIP assay kit with modifications. In brief, LNCaP cells were cultured in 5% FBS-RPMI and treated with 10 nM 1,25-$(OH)_2D_3$ overnight. After cellular chromatin cross-linking with 1% formaldehyde, chromatin pellets were sonicated to an average of 200- to 1000-bp fragments of DNA. The chromatin fragments were subjected to immunoprecipitation with the 2 μg of polyclonal antisera to VDR or RXRα (65) (Santa Cruz Biotechnology) overnight at 4 C. The precipitates were eluted into the elution buffer containing 1% SDS, 100 mM $NaHCO_3$, and 10 mM DTT. The cross-links were reversed with a 4-h incubation at 65 C in the elution buffer with addition of 200 mM NaCl. The immunoprecipitated DNA fragments were purified using QIAGEN MiniElute Reaction Cleanup kits and subjected to PCR using a pair of primers (upper, 5′-TGACCACACCGACAGGTTTG-3′; lower, 5′-ATTTCACAGGCTGGCTGGAGTG-3′), which were designed to amplify the IGFBP-3 promoter sequence from −3340 to −3207 containing BP3-VDRE and give rise to a 134-bp fragment. The DyNAmo SYBR Green qPCR kit (MJ Research Inc., South San Francisco, CA) was used in the PCR. PCR was carried out as follows: 95 C for 5 min, then 35 cycles of 94 C for 20 sec, 58 C for 20 sec, and 72 C for 30 sec with a final extension for 6 min at 72 C. PCR products were separated on 2.5% agarose gels and visualized with ethidium bromide staining.

Acknowledgments

Received September 8, 2003. Accepted February 6, 2004.

Address all correspondence and requests for reprints to: Dr. David Feldman, Division of Endocrinology, Department of Medicine, Stanford University School of Medicine, Stanford, California 94305-5103. E-mail: feldman@cmgm.stanford.edu.

This work was supported by Department of Army Grant DAMD17-02-1-0142, National Institutes of Health Grant DK 42482, and CAP CURE.

REFERENCES

1. Feldman D, Malloy PJ, Gross C 2001 Vitamin D: biology, action and clinical implications. In: Marcus R, Feldman D, Kelsey J, eds. Osteoporosis. 2nd ed. San Diego: Academic Press; 257–303
2. Gross C, Peehl DM, Feldman D 1997 Vitamin D and prostate cancer. In: Feldman D, Glorieux FH, Pike JW, eds. Vitamin D. San Diego: Academic Press; 1125–1139
3. Miller GJ 1998 Vitamin D and prostate cancer: biologic interactions and clinical potentials. Cancer Metastasis Rev 17:353–360
4. Blutt SE, Weigel NL 1999 Vitamin D and prostate cancer. Proc Soc Exp Biol Med 221:89–98
5. Konety BR, Johnson CS, Trump DL, Getzenberg RH 1999 Vitamin D in the prevention and treatment of prostate cancer. Semin Urol Oncol 17:77–84
6. Krishnan AV, Peehl DM, Feldman D 2003 The role of vitamin D in prostate cancer. Recent Results Cancer Res 164:205–221
7. Peehl DM, Krishnan AV, Feldman D 2003 Pathways mediating the growth-inhibitory actions of vitamin D in prostate cancer. J Nutr 133:2461S–2469S
8. Zhuang SH, Burnstein KL 1998 Antiproliferative effect of 1α,25-dihydroxyvitamin D3 in human prostate cancer cell

line LNCaP involves reduction of cyclin-dependent kinase 2 activity and persistent G1 accumulation. Endocrinology 139:1197–1207
9. Blutt SE, McDonnell TJ, Polek TC, Weigel NL 2000 Calcitriol-induced apoptosis in LNCaP cells is blocked by overexpression of Bcl-2. Endocrinology 141:10–17
10. Bernard D, Pourtier-Manzanedo A, Gil J, Beach DH 2003 Myc confers androgen-independent prostate cancer cell growth. J Clin Invest 112:1724–1731
11. Liu M, Lee MH, Cohen M, Bommakanti M, Freedman LP 1996 Transcriptional activation of the Cdk inhibitor p21 by vitamin D3 leads to the induced differentiation of the myelomonocytic cell line U937. Genes Dev 10:142–153
12. Blutt SE, Allegretto EA, Pike JW, Weigel NL 1997 1,25-Dihydroxyvitamin D3 and 9-cis-retinoic acid act synergistically to inhibit the growth of LNCaP prostate cells and cause accumulation of cells in G1. Endocrinology 138:1491–1497
13. Rajah R, Valentinis B, Cohen P 1997 Insulin-like growth factor (IGF)-binding protein-3 induces apoptosis and mediates the effects of transforming growth factor-β1 on programmed cell death through a p53- and IGF-independent mechanism. J Biol Chem 272:12181–12188
14. Colston KW, Perks CM, Xie SP, Holly JM 1998 Growth inhibition of both MCF-7 and Hs578T human breast cancer cell lines by vitamin D analogues is associated with increased expression of insulin-like growth factor binding protein-3. J Mol Endocrinol 20:157–162
15. Huynh H, Pollak M, Zhang JC 1998 Regulation of insulin-like growth factor (IGF) II and IGF binding protein 3 autocrine loop in human PC-3 prostate cancer cells by vitamin D metabolite 1,25(OH)2D3 and its analog EB1089. Int J Oncol 13:137–143
16. Boyle BJ, Zhao XY, Cohen P, Feldman D 2001 Insulin-like growth factor binding protein-3 mediates 1α,25-dihydroxyvitamin D(3) growth inhibition in the LNCaP prostate cancer cell line through p21/WAF1. J Urol 165: 1319–1324
17. Krishnan AV, Peehl DM, Feldman D 2003 Inhibition of prostate cancer growth by vitamin D: regulation of target gene expression. J Cell Biochem 88:363–371
18. Chan JM, Stampfer MJ, Giovannucci E, Gann PH, Ma J, Wilkinson P, Hennekens CH, Pollak M 1998 Plasma insulin-like growth factor-I and prostate cancer risk: a prospective study. Science 279:563–566
19. Harman SM, Metter EJ, Blackman MR, Landis PK, Carter HB 2000 Serum levels of insulin-like growth factor I (IGF-I), IGF-II, IGF-binding protein-3, and prostate-specific antigen as predictors of clinical prostate cancer. J Clin Endocrinol Metab 85:4258–4265
20. Stattin P, Bylund A, Rinaldi S, Biessy C, Dechaud H, Stenman UH, Egevad L, Riboli E, Hallmans G, Kaaks R 2000 Plasma insulin-like growth factor-I, insulin-like growth factor-binding proteins, and prostate cancer risk: a prospective study. J Natl Cancer Inst 92:1910–1917
21. Chokkalingam AP, Pollak M, Fillmore CM, Gao YT, Stanczyk FZ, Deng J, Sesterhenn IA, Mostofi FK, Fears TR, Madigan MP, Ziegler RG, Fraumeni Jr JF, Hsing AW 2001 Insulin-like growth factors and prostate cancer: a population-based case-control study in China. Cancer Epidemiol Biomarkers Prev 10:421–427
22. Stattin P, Stenman UH, Riboli E, Hallmans G, Kaaks R 2001 Ratios of IGF-I, IGF binding protein-3, and prostate-specific antigen in prostate cancer detection. J Clin Endocrinol Metab 86:5745–5748
23. Chan JM, Stampfer MJ, Ma J, Gann P, Gaziano JM, Pollak M, Giovannucci E 2002 Insulin-like growth factor-I (IGF-I) and IGF binding protein-3 as predictors of advanced-stage prostate cancer. J Natl Cancer Inst 94: 1099–1106
24. Sarma AV, Jaffe CA, Schottenfeld D, Dunn R, Montie JE, Cooney KA, Wei JT 2002 Insulin-like growth factor-1, insulin-like growth factor binding protein-3, and body mass index: clinical correlates of prostate volume among Black men. Urology 59:362–367
25. Baxter RC, Martin JL 1989 Structure of the Mr 140,000 growth hormone-dependent insulin-like growth factor binding protein complex: determination by reconstitution and affinity-labeling. Proc Natl Acad Sci USA 86: 6898–6902
26. Hwa V, Oh Y, Rosenfeld RG 1999 The insulin-like growth factor-binding protein (IGFBP) superfamily. Endocr Rev 20:761–787
27. Rajah R, Khare A, Lee PD, Cohen P 1999 Insulin-like growth factor-binding protein-3 is partially responsible for high-serum-induced apoptosis in PC-3 prostate cancer cells. J Endocrinol 163:487–494
28. Leal SM, Liu Q, Huang SS, Huang JS 1997 The type V transforming growth factor β receptor is the putative insulin-like growth factor-binding protein 3 receptor. J Biol Chem 272:20572–20576
29. Schedlich LJ, Le Page SL, Firth SM, Briggs LJ, Jans DA, Baxter RC 2000 Nuclear import of insulin-like growth factor-binding protein-3 and -5 is mediated by the importin beta subunit. J Biol Chem 275:23462–23470
30. Liu B, Lee HY, Weinzimer SA, Powell DR, Clifford JL, Kurie JM, Cohen P 2000 Direct functional interactions between insulin-like growth factor-binding protein-3 and retinoid X receptor-α regulate transcriptional signaling and apoptosis. J Biol Chem 275:33607–33613
31. Lee KW, Liu B, Ma L, Li H, Bang P, Koeffler HP, Cohen P 2004 Cellular internalization of insulin-like growth factor binding protein-3: distinct endocytic pathways facilitate re-uptake and nuclear localization. J Biol Chem 279:469–476
32. Oh Y, Muller HL, Ng L, Rosenfeld RG 1995 Transforming growth factor-β-induced cell growth inhibition in human breast cancer cells is mediated through insulin-like growth factor-binding protein-3 action. J Biol Chem 270: 13589–13592
33. Huynh H, Nickerson T, Pollak M, Yang X 1996 Regulation of insulin-like growth factor I receptor expression by the pure antiestrogen ICI 182780. Clin Cancer Res 2:2037–2042
34. Rozen F, Zhang J, Pollak M 1998 Antiproliferative action of tumor necrosis factor-α on MCF-7 breast cancer cells is associated with increased insulin-like growth factor binding protein-3 accumulation. Int J Oncol 13:865–869
35. Tsubaki J, Choi WK, Ingermann AR, Twigg SM, Kim HS, Rosenfeld RG, Oh Y 2001 Effects of sodium butyrate on expression of members of the IGF-binding protein superfamily in human mammary epithelial cells. J Endocrinol 169:97–110
36. Pratt SE, Pollak MN 1993 Estrogen and antiestrogen modulation of MCF7 human breast cancer cell proliferation is associated with specific alterations in accumulation of insulin-like growth factor-binding proteins in conditioned media. Cancer Res 53:5193–5198
37. Buckbinder L, Talbott R, Velasco-Miguel S, Takenaka I, Faha B, Seizinger BR, Kley N 1995 Induction of the growth inhibitor IGF-binding protein 3 by p53. Nature 377:646–649
38. Gucev ZS, Oh Y, Kelley KM, Rosenfeld RG 1996 Insulin-like growth factor binding protein 3 mediates retinoic acid- and transforming growth factor β2-induced growth inhibition in human breast cancer cells. Cancer Res 56: 1545–1550
39. Haussler MR, Whitfield GK, Haussler CA, Hsieh JC, Thompson PD, Selznick SH, Dominguez CE, Jurutka PW 1998 The nuclear vitamin D receptor: biological and molecular regulatory properties revealed. J Bone Miner Res 13:325–349
40. Freedman LP 1999 Increasing the complexity of coactivation in nuclear receptor signaling. Cell 97:5–8
41. Takeyama K, Masuhiro Y, Fuse H, Endoh H, Murayama A, Kitanaka S, Suzawa M, Yanagisawa J, Kato S 1999

Selective interaction of vitamin D receptor with transcriptional coactivators by a vitamin D analog. Mol Cell Biol 19:1049–1055
42. Cubbage ML, Suwanichkul A, Powell DR 1990 Insulin-like growth factor binding protein-3. Organization of the human chromosomal gene and demonstration of promoter activity. J Biol Chem 265:12642–12649
43. Zierold C, Darwish HM, DeLuca HF 1995 Two vitamin D response elements function in the rat 1,25-dihydroxyvitamin D 24-hydroxylase promoter. J Biol Chem 270: 1675–1678
44. Zierold C, Darwish HM, DeLuca HF 1994 Identification of a vitamin D-response element in the rat calcidiol (25-hydroxyvitamin D3) 24-hydroxylase gene. Proc Natl Acad Sci USA 91:900–902
45. Kerry DM, Dwivedi PP, Hahn CN, Morris HA, Omdahl JL, May BK 1996 Transcriptional synergism between vitamin D-responsive elements in the rat 25-hydroxyvitamin D3 24-hydroxylase (CYP24) promoter. J Biol Chem 271: 29715–29721
46. Nordeen SK, Ogden CA, Taraseviciene L, Lieberman BA 1998 Extreme position dependence of a canonical hormone response element. Mol Endocrinol 12:891–898
47. Kerner SA, Scott RA, Pike JW 1989 Sequence elements in the human osteocalcin gene confer basal activation and inducible response to hormonal vitamin D3. Proc Natl Acad Sci USA 86:4455–4459
48. Morrison NA, Shine J, Fragonas JC, Verkest V, McMenemy ML, Eisman JA 1989 1,25-dihydroxyvitamin D-responsive element and glucocorticoid repression in the osteocalcin gene. Science 246:1158–1161
49. Demay MB, Gerardi JM, DeLuca HF, Kronenberg HM 1990 DNA sequences in the rat osteocalcin gene that bind the 1,25-dihydroxyvitamin D3 receptor and confer responsiveness to 1,25-dihydroxyvitamin D3. Proc Natl Acad Sci USA 87:369–373
50. Markose ER, Stein JL, Stein GS, Lian JB 1990 Vitamin D-mediated modifications in protein-DNA interactions at two promoter elements of the osteocalcin gene. Proc Natl Acad Sci USA 87:1701–1705
51. Noda M, Vogel RL, Craig AM, Prahl J, DeLuca HF, Denhardt DT 1990 Identification of a DNA sequence responsible for binding of the 1,25-dihydroxyvitamin D3 receptor and 1,25-dihydroxyvitamin D3 enhancement of mouse secreted phosphoprotein 1 (SPP-1 or osteopontin) gene expression. Proc Natl Acad Sci USA 87: 9995–9999
52. Ozono K, Liao J, Kerner SA, Scott RA, Pike JW 1990 The vitamin D-responsive element in the human osteocalcin gene. Association with a nuclear proto-oncogene enhancer. J Biol Chem 265:21881–1888
53. MacDonald PN, Haussler CA, Terpening CM, Galligan MA, Reeder MC, Whitfield GK, Haussler MR 1991 Baculovirus-mediated expression of the human vitamin D receptor. Functional characterization, vitamin D response element interactions, and evidence for a receptor auxiliary factor. J Biol Chem 266:18808–18813
54. Hijiya N, Setoguchi M, Matsuura K, Higuchi Y, Akizuki S, Yamamoto S 1994 Cloning and characterization of the human osteopontin gene and its promoter. Biochem J 303:255–262
55. Cao X, Ross FP, Zhang L, MacDonald PN, Chappel J, Teitelbaum SL 1993 Cloning of the promoter for the avian integrin β 3 subunit gene and its regulation by 1,25-dihydroxyvitamin D3. J Biol Chem 268:27371–27380
56. Ohyama Y, Ozono K, Uchida M, Shinki T, Kato S, Suda T, Yamamoto O, Noshiro M, Kato Y 1994 Identification of a vitamin D-responsive element in the 5′-flanking region of the rat 25-hydroxyvitamin D3 24-hydroxylase gene. J Biol Chem 269:10545–10550
57. Chen KS, DeLuca HF 1995 Cloning of the human 1α,25-dihydroxyvitamin D-3 24-hydroxylase gene promoter and identification of two vitamin D-responsive elements. Biochim Biophys Acta 1263:1–9
58. Gill RK, Christakos S 1993 Identification of sequence elements in mouse calbindin-D28k gene that confer 1,25-dihydroxyvitamin D3- and butyrate-inducible responses. Proc Natl Acad Sci USA 90:2984–2988
59. Eelen G, Verlinden L, Camp MV, Hummelen PV, Marchal K, Moor BD, Mathieu C, Carmeliet G, Bouillon R, Verstuyf A 2004 The effects of 1α,24-dihydroxyvitamin D3 on the expression of DNA replication genes. J Bone Miner Res 19:133–146
60. Lee KW, Cohen P 2002 Nuclear effects: unexpected intracellular actions of insulin-like growth factor binding protein-3. J Endocrinol 175:33–40
61. Malloy PJ, Hochberg Z, Tiosano D, Pike JW, Hughes MR, Feldman D 1990 The molecular basis of hereditary 1,25-dihydroxyvitamin D3 resistant rickets in seven related families. J Clin Invest 86:2071–2079
62. Malloy PJ, Xu R, Peng L, Clark PA, Feldman D 2002 A novel mutation in helix 12 of the vitamin D receptor impairs coactivator interaction and causes hereditary 1,25-dihydroxyvitamin D-resistant rickets without alopecia. Mol Endocrinol 16:2538–2546
63. Kimmel-Jehan C, Jehan F, DeLuca HF 1997 Salt concentration determines 1,25-dihydroxyvitamin D3 dependency of vitamin D receptor-retinoid X receptor-vitamin D-responsive element complex formation. Arch Biochem Biophys 341:75–80
64. Peng L, Payne AH 2002 AP-2 γ and the homeodomain protein distal-less 3 are required for placental-specific expression of the murine 3 β-hydroxysteroid dehydrogenase VI gene, Hsd3b6. J Biol Chem 277:7945–7954
65. Yamamoto H, Shevde NK, Warrier A, Plum LA, DeLuca HF, Pike JW 2003 2-Methylene-19-nor-(20S)-1,25-dihydroxyvitamin D3 potently stimulates gene-specific DNA binding of the vitamin D receptor in osteoblasts. J Biol Chem 278:31756–31765

Molecular Endocrinology is published monthly by The Endocrine Society (http://www.endo-society.org), the foremost professional society serving the endocrine community.